This document is the accepted manuscript version of the following article:
Chen, J., Jacques, S., Barthe, M. F., Zhang, C., & Desgardin, P. (2020). In-beam creep of SiCf/SiC minicomposites under uniaxial tensile loading. Journal of Nuclear Materials, 533, 152086 (7 pp.).
https://doi.org/10.1016/j.jnucmat.2020.152086

In-beam creep of SiC_f/SiC minicomposites under uniaxial tensile loading

Jiachao Chen[1], Sylvain Jacques[2], Marie-France Barthe[3], Chonghong Zhang[4], Pierre Desgardin[3]

[1]*Department of Nuclear Energy and Safety, Paul Scherrer Institute, 5232 Villigen PSI, Switzerland*
[2]*Laboratoire des Composites Thermostructuraux, CNRS/University of Bordeaux, 33600 Pessac, France*
[3]*CEMHTI/CNRS, Université d'Orléans, 3A rue de la Férollerie, 45071 Orléans CEDEX 2, France*
[4]*Institute of Modern Physics, Chinese Academy of Science, Lanzhou, China*

A newly developed clamping system for ceramic specimen is described in the present report. By using this system, the uniaxial tensile loading was first successfully applied up to fracture (950 MPa) on a SiC_f/SiC minicomposite. A minicomposite is a 1D model composite. It consists of a SiC-based fiber tow embedded in a SiC matrix, which has a diameter of about 0.5 mm. Afterwards, the irradiation creep properties of SiC_f/SiC minicomposites were studied. In-situ creep was performed in an in-beam creep device under uniaxial tensile stresses from 40 to 382 MPa during homogeneous helium irradiation. Homogenous irradiation was carried out by helium implantation with energies varying from 0 to 45 MeV. The displacement dose rate was 1.2×10^{-6} dpa/s. The average temperature was controlled to 700 and 900°C within ±15°C. Irradiation creep compliance of minicomposite was measured to be 3.07×10^{-5} and 5.43×10^{-5} dpa^{-1} MPa^{-1} at 700°C and 900°C, respectively.

Key words:
SiC_f/SiC composite, high-temperature mechanical testing, irradiation creep, clamping system

*Corresponding author:
Jiachao Chen
Paul Scherrer Institut
CH-5232 Villigen PSI
Switzerland
Tel: +41 56 310 2280; fax: +41 56 310 4595
E-mail address: jiachao.chen@psi.ch

1. Introduction

Besides ITER as the key pilot fusion device toward future fusion power plants [1], several concepts for future nuclear fission plants were proposed as well within the framework of the international Generation IV Initiative Forum (GIF) [2] and of the Sustainable Nuclear Energy Technology Platform (SNETP) in Europe [3]. Different to current light water reactors (LWR), both fusion and Generation IV Reactors will operate at much more extreme conditions, including high temperatures, high stresses, and high irradiation doses. However, to realize these advanced nuclear plants, development of high performance materials (structural and fuel) in such environments is a key issue.

Silicon carbide (SiC) fiber reinforced SiC matrix composites (SiC_f/SiC) have an excellent retention of mechanical properties, chemical and environmental inertness at high temperature, inherently low activation properties in neutron radiation environments. They are therefore considered as promising potential materials for first wall and blanket in the fusion reactor system [4, 5] and candidate cladding materials for advanced high temperature gas cooled fast reactors [6], where in some accident scenarios the cladding temperature can rise to 1600°C. Following the Fukushima accident, SiC_f/SiC composites are also considered as cladding materials for enhanced accident-tolerant fuels (ATF) of light water reactor (LWRs) [7, 8]. The proposed cladding shapes are the plate design with internal hexagonal cells, containing the fuel, or a conventional cylindrical shape [9]. In both cases the cladding has to withstand stress from swelling/expanding fuel, and formation of fission gas. Irradiation creep is one of the major processes by which the dimensional stability of structural components can be altered during radiation exposure, and its control is therefore crucial for cladding performance. However, it is believed that the fibers are less creep resistant than the matrix, which make the fibers sensitive to the phenomenon of delayed failure by a mechanism called slow or sub-critical crack growth [10] and lead to a decrease in the mechanical strength of the composite or even to its failure.

Because of technical difficulty, there is only a scarce database on irradiation creep of monolithic SiC, SiC fiber and SiC_f/SiC composites [11-17]. By applying bend stress relaxation (BSR) methods, irradiation creep of monolithic SiC and SiC_f/SiC composites has been investigated under neutron irradiation in a nuclear reactor [11, 15, 17]. Meanwhile

irradiation creep of SiC fibers have been studied by torsion method [12] and BSR method [13] under proton beam irradiation. Obviously, BRS and torsion methods have their disadvantages. Due to inhomogeneous strain/stress distribution in the samples, the analysis of the results is quite complex, especially when the exponent of stress is not equal to one and/or the irradiation creep experiences a transition stage during exposure. It is worth mentioning that irradiation creep of thin strip specimen of chemically vapor-deposited (CVD) monolithic SiC has been studied under tensile load during the penetrating proton irradiation [14]. In reference [14], the maximum tensile load reached 98 MPa still far below fracture stress and the strain measurement is still not precise enough to monitor the details of strain-dose curve, which is the main advantage of in situ experiments. Therefore, a new clamping system that can be adapted to an existing cyclotron-based irradiation creep device was designed for ceramic specimens. By using this system, irradiation creep of a SiC_f/SiC composite under uniaxial tensile loading was investigated and discussed in regard with literature data.

2. Experiments

2.1 Materials and samples

The samples used in this study were SiC_f/SiC minicomposites. They were manufactured at the laboratory for thermostructural composites (LCTS), CNRS/University of Bordeaux, France. A minicomposite is a 1D model composite [18]. It consists of one fiber tow in which a thin pyrocarbon coating called “interphase” and then the SiC matrix are infiltrated by chemical vapor infiltration (CVI) methods derived from CVD. The interphase makes it possible to obtain tough composites despite the brittleness of the ceramic components. The gas method used produces materials of very high purity. The tow is composed of 500 Hi-Nicalon S fibers (monofilaments, ~12 μm in diameter, from Nippon Carbon, Japan) (Fig. 1). These last generation fibers are referred to as “near-stoichiometric SiC fibers”. The geometry of the minicomposite is simpler than that of the actual composite. It can properly represent its behavior and, specially, its small size (0.5 mm in diameter and 32 mm in length) is well suited for the present irradiation creep experiments.

The interphase and the matrix were successively infiltrated into fiber tows at low pressure and at a temperature of about 1000°C in the same hot wall reactor. Propane was the gas precursor for the pyrocarb on interphase. The interphase coating thickness was estimated at

30-40 nm from the deposition time and rate. The SiC matrix was infiltrated from a gaseous mixture of methiltrichlorosilane and hydrogen. The matrix volume fraction of the processed minicomposites were measured by weighing without taking into account porosity, it is 0.69.

2.2 Clamping system for ceramic specimen

The in-situ irradiation device, originally developed by FzJ [19,20] and modified by PSI, installed at CEMHTI/CNRS was employed for the present experiment. The irradiation creep of the SiC_f/SiC composite is a technical challenge. The clamping system developed for metal samples does not work properly for ceramics. The sample is fixed by forced mechanical contact in traditional clamping system. Looking more closely, such contact between sample and sample holder actually occurs at several points. The real stress applied on the sample at the contact point are very high. The ceramic cannot have local plastic deformation to mitigate such stress at low temperature but the metal samples do. This could be the reason that traditional clamping system does not work properly for ceramic. To avoid the forced mechanical contact between sample and sample holder, a new clamping system for ceramic was therefore designed. Minicomposites were glued with alumina-based glue (Ceramabond® 503 from Aremco) in the graphite grips, which were fixed to the metal frame. The ensemble could be mounted in the loading parts of in situ irradiation creep device. The glue was cured in air by incremental heat treatment up to a temperature of ~370°C according to the manufacturer's instructions. During the heat treatment, the screws of one of the two graphite grips were removed from the mounting to avoid sample damages due to metal thermal expansion. The graphite block could stand for high temperature, could be fixed mechanically to the metal frame without broken, and could protect metal pieces against overheating. The overall schematic view of the specimen holder for irradiation creep test of ceramics is showed in Fig. 2.

2.3 Irradiation

In-beam creep tests under He-irradiation were performed at the cyclotron of CEMHTI (Conditions Extrêmes et Matériaux: Haute Température et Irradiation)/CNRS (Centre National de la Recherche Scientifique) under support of the French Network EMIR (Réseau national d'accélérateurs pour les Etudes des Matériaux sous Irradiation) and the NEEDS

(Nucléaire, énergie, environnement, déchets, société) programme. A sketch of the experimental set up is illustrated in Fig. 3. With 45 MeV $_4He^{2+}$ ions passing through firstly a magnet scanning system which create a Lissajous scanning, then a vacuum window of a 25 µm thick Hastelloy foil, and finally a degrader wheel with 30 Al-foils of various thicknesses, the 0.5 mm thick samples were 3D-homogeneously irradiated/implanted under constant uniaxial stress. The specimens were loaded by a motor driven spring, with the specimen clamps moving in a guiding frame to avoid any torsion. The production of displacement damage was calculated by TRIM and SRIM for a displacement threshold energy of 35 and 20 eV for Si and C atoms, respectively; and a binding energy of 3.25 and 2.63 eV for Si and C atoms, respectively [21, 22]. The displacement damage profile in SiC sample is shown in Fig. 4. Typical displacement damage rate was $1.2x10^{-6}$ dpa/s (displacement per atom per second) with a concurrently helium implantation rate of 0.0067 appm-He/s (atomic parts per million per second) if the aperture was 4 mm x12 mm and beam current was 5 µA after aperture window. The desired specimen temperature was obtained by cooling the samples via controlled jets (5 on the right and 5 on the left side of the sample) of purified helium gas. The temperature distribution along the sample was monitored by an infrared pyrometer under 45° from the backside of the specimens during irradiation (see Fig. 5). The geometrical center of the sample is defined as position of origin (0 position), and up direction is positive. The region irradiated by beam located between two arrows (from position -6 to 6). The emissivity value of SiC_f/SiC composites was chosen as 0.8 [23]. The temperature fluctuation during irradiation was ±15°C. The temperature fluctuation during beam-on directly leads the length changes of samples that is much larger than the elongation induced by irradiation in the present experiment conditions. Therefore, the elongation of specimens was monitored by two LVDT (Linear Variable Differential Transformer) positioned on both sides of the specimen under constant load in the period of beam-off. The irradiation continued until the strain rate became constant (stationary creep). Then, irradiation of the same specimen was resumed at a different stress in the range of 40 to 382 MPa.

3. Results and discussion

To check the feasibility of the new clamping system, a trial tensile test was performed at 900°C under beam heating. A typical tensile curve of SiC_f/SiC composites is shown in the fig. 6. The insert of photo in Fig. 6 shows fractured specimen after tensile test. From the plot, uniaxial

tensile loading was first applied up to fracture of 950 MPa and SiC_f/SiC composite specimen failed in the center region. It demonstrates that this new clamping system is successful. According to our tensile curve, below 400 MPa there is a complete absence of sample sliding and pseudo-plastic deformation. The stress applied for creep tests will be remained below 400 MPa.

Because of different thermal expansion coefficient of specimen holder, support parts and sample itself, the measured length change by LVDT depends on the temperature distribution in the chamber. Therefore, in order to improve data precision, all strains have to be taken at a constant chamber temperature. One example is illustrated in Fig. 7. The strain measurements were taken at 65°C and a precision of < 0.1 µm (corresponding to the strain resolution of better than 10^{-5}) was achieved.

Fig.8 and 9 show the strain of SiC_f/SiC minicomposite during He-irradiation at 700°C and 900°C as a function of the displacement dose, respectively. Each stress change caused, aside from elastic strain, also a short transient stage before stationary creep was reached. Those transient strains are similar to observations in steels [24, 25]. They are ascribed to irradiation-induced relaxation or transient irradiation creep. It is worth mentioning that a contraction of the specimen against the applied tensile stress occurred at the beginning of irradiation when the applied stress was reduced (e.g. from 280 MPa to 101 MPa at 700°C and from 382 to 93 MPa at 900°C). Nevertheless, already after a dose of less than 0.03 dpa, creep proceeds again in the stress direction. The mechanism of the transient irradiation creep is not clear yet. Hesketh [26] has proposed a model to describe this phenomenon. The basic idea is that vacancies and interstitials created by irradiation give rise to a chemical stress on dislocation. Pinned dislocation lines climb to form the bows under this chemical stress. Such dislocation bows randomly and homogenously distributed in the all-possible lattice directions. External stress will cause preferential arrangement of the bows in sizes resulting a final creep strain, which is proportional to stress, and independent of temperature. Afterwards, a steady state irradiation creep follows up. When applied stress changes, the rearrangement of those bows leads such transient creep strain, i.e. contraction or expansion depending on stress change directions. According to results from thermal creep test, it is fair to conclude that thermal creep is negligible at $T \leq 1000$°C [27]. The measured length change is sum of irradiation creep and defect swelling as described by equation (1).

$$\varepsilon'_{total}(\sigma,\phi) = \varepsilon'_{swelling}(\phi) + \varepsilon'_{creep}(\sigma,\phi) \quad (1)$$

Where ε'_{total}, $\varepsilon'_{swelling}$ and ε'_{creep} are measured total strain rate, strain rate due to defect swelling i.e. swelling strain/damage dose (in unit of dpa^{-1}), and strain rate due to irradiation creep i.e. irradiation creep strain rate/damage rate (in unit of dpa^{-1}). σ , ϕ are applied stress and damage dose, respectively. If strain rate reaches the steady state and keep a linear relationship with the irradiation flux [12], then:

$$\varepsilon'_{total}(\sigma,\phi) = \varepsilon'_{swelling}(\phi) + B_0 \cdot \sigma \quad (2)$$

Where B_0 denotes irradiation creep compliance. Published data on irradiation creep of SiC demonstrated a linear stress dependence of the irradiation creep rate [11-17].
Irradiation-induced total strain rates, i.e. strain-rate per dose-rate (in unit of dpa^{-1}) were obtained by fitting straight lines to the stationary parts of the curves in Fig. 8 and 9. These values of $\varepsilon'_{total}(\sigma,\phi)$ are plotted in Fig. 10 as a function of the applied stress (σ) for both temperatures. The number close to the measurement point in Fig. 10 indicates the measuring sequences. Because $\varepsilon'_{swelling}(\phi)$ smoothly and monotonously decreases down to zero (due to the saturation of defect swelling in SiC) in high dose at temperature below 1000°C [28, 29]. The swelling contribution in measured total strain rate should continuously decrease with increasing damage dose. Accordingly, irradiation creep compliance can be measured by changing the applied stress alternately to higher and lower values. Here a detailed explanation is given. At 700°C, the applied stresses designed in a sequence (see Fig. 8) of σ_1=40 MPa (M-1), σ_2=280 MPa (M-2), σ_3=101 MPa (M-3) and σ_4=280 MPa (M-4). According to the Eq (2), the measured strains of 4 points at 700°C could be described by

$$\varepsilon'_{total}(\sigma_1,\phi_1) = \varepsilon'_{swelling}(\phi_1) + B_0 \cdot \sigma_1 \quad (3)$$

$$\varepsilon'_{total}(\sigma_2,\phi_2) = \varepsilon'_{swelling}(\phi_2) + B_0 \cdot \sigma_2 \quad (4)$$

$$\varepsilon'_{total}(\sigma_3,\phi_3) = \varepsilon'_{swelling}(\phi_3) + B_0 \cdot \sigma_3 \quad (5)$$

$$\varepsilon'_{total}(\sigma_4,\phi_4) = \varepsilon'_{swelling}(\phi_4) + B_0 \cdot \sigma_4 \quad (6)$$

The numbers in the subscript position of σ (stress) and ϕ (dose) symbols in the equations (3) to (9) indicate the measuring sequences. Since the swelling portion is high at measurement M-1 which can cause large error, we take measurement M-2, M-3 and M-4 to extract the B_0

Subtracting eq (4) to eq (5) and eq(6) to eq (5), one obtains:

$$B_0 = \frac{\varepsilon'_{total}(\sigma_2, \phi_2) - \varepsilon'_{total}(\sigma_3, \phi_3)}{\sigma_2 - \sigma_3} - \frac{\varepsilon'_{swelling}(\phi_2) - \varepsilon'_{swelling}(\phi_3)}{\sigma_2 - \sigma_3} \quad (7)$$

$$B_0 = \frac{\varepsilon'_{total}(\sigma_4, \phi_4) - \varepsilon'_{total}(\sigma_3, \phi_3)}{\sigma_4 - \sigma_3} - \frac{\varepsilon'_{swelling}(\phi_4) - \varepsilon'_{swelling}(\phi_3)}{\sigma_4 - \sigma_3} \quad (8)$$

Because $\varepsilon'_{swelling}(\phi)$ smoothly and monotonously decreases down to zero (due to the saturation of defect swelling in SiC) in high dose at temperature below 1000°C [27, 28], then:

$$\varepsilon'_{swelling}(\phi_2) > \varepsilon'_{swelling}(\phi_3) > \varepsilon'_{swelling}(\phi_4)$$

One obtains the second term in eq (7) $\frac{\varepsilon'_{swelling}(\phi_2) - \varepsilon'_{swelling}(\phi_3)}{\sigma_2 - \sigma_3} > 0$; and in eq (8) $\frac{\varepsilon'_{swelling}(\phi_4) - \varepsilon'_{swelling}(\phi_3)}{\sigma_4 - \sigma_3} < 0$

therefore

$$\frac{\varepsilon'_{total}(\sigma_4, \phi_4) - \varepsilon'_{total}(\sigma_3, \phi_3)}{\sigma_4 - \sigma_3} < B_0 < \frac{\varepsilon'_{total}(\sigma_2, \phi_2) - \varepsilon'_{total}(\sigma_3, \phi_3)}{\sigma_2 - \sigma_3} \quad (9)$$

The right term in eq (9), $\frac{\varepsilon'_{total}(\sigma_2, \phi_2) - \varepsilon'_{total}(\sigma_3, \phi_3)}{\sigma_2 - \sigma_3}$ and the left term in eq (9), $\frac{\varepsilon'_{total}(\sigma_4, \phi_4) - \varepsilon'_{total}(\sigma_3, \phi_3)}{\sigma_4 - \sigma_3}$ are the slopes of the lines connecting M-3 and M-2; and connecting M-3 and M-4, respectively.

Conclusively, the slope of straight line connecting M-3 and M-2 (short dash) gives an upper limit of irradiation creep compliance. On the other hand, slope of straight line connecting M-3 and M-4 (short dash) gives a lower limit. The correct one should be a slope between above-

mentioned two slopes as indicated by solid line fitting to measurement M-2, 3 and 4 (red square) in the Fig. 10. From measured data, the swelling contribution at 700°C is significant at beginning of irradiation but decreases quite quickly with dose. At 900°C, the strain rate at 93 MPa (M-4) cannot be extracted since the last part of strain-dose curve stopped within transient stage. Fortunately, the data (black circle) can be fitted by linear stress dependence with an offset close to 0 up to 382 MPa at 900°C (dashed line). This indicates that swelling at 900°C is negligible. The creep compliances B_0, i.e. creep rate per dose rate were determined as 3.07×10^{-5} $dpa^{-1} \cdot MPa^{-1}$ and 5.43×10^{-5} $dpa^{-1} \cdot MPa^{-1}$ at temperature of 700°C and 900°C, respectively.

Similar to metal and steels, irradiation creep of SiC and its composites under constant load is believed to exhibit primary transient creep followed by steady-state creep with increasing irradiation damage dose. There are very limited in situ experiment in studying irradiation creep behavior [12, 14], where the strain-dose curves under stress could be measured. In ref. [14], recorded strain-dose curve under stress does not show the details due to poor resolution of strain measurement. Irradiation creep of SCS-6 fiber were characterized by transients below 0.05 dpa at 600°C by in situ torsion experiment as reported in Ref. [12]. In present study, strain-dose curves under applied stress demonstrates that transient creep remains up to 0.02 – 0.05 dpa even affected by the history of applied stress.

Irradiation creep compliance of various experiments, i.e. from different irradiation environments, different loading states are summarized in Fig. 11. All data divided in three displacement dose regimes, i.e. 0.01-0.1 dpa, 0.1-1 dpa and above 1 dpa indicated by empty (black), x-hair (red) and filled symbols (blue), respectively. Measurable irradiation creep starts from 400°C (symbols located in the abscissa mean that no irradiation creep stress could be measured). Meanwhile it was reported no stress dependence of strain of SiC under tensile loading up to 100 MPa at temperature range of 235-505°C [30]. It is worth mentioning that by keeping all other parameters constant, the torsion method gives a higher creep compliance under irradiation than the BSR technique in spite only one data point. The measured irradiation compliance scatted in wide orders of magnitude. This discrepancy can possibly arise from the following reasons:

1) In all neutron irradiation study, the conversion factor of 1 dpa = 1.0×10^{25} n/m^2 (E > 0.1 MeV) is applied which overestimate the dpa number according to the suggested conversion factor of 1 dpa = 6.3×10^{25} n/m^2 (E > 0.1 MeV) [21]. Light ions and

neutrons (and heavy ions) produce different recoil spectrum, which have a different efficiency of defect production. Calculations based on NRT model overestimate the efficiency of defect production of neutrons by about a factor of three [31] in metal. Considering above-mentioned reasons, irradiation creep compliance has been measured too low in the neutron irradiation investigation.

2) There are some indications [32] that irradiation creep rates in bending test may be slightly lower than uniaxial loading. Especially, the sample suffered continuous decreasing stress during irradiation by BSR method that may cause uncompleted transient stage in the whole irradiation period. This results in a lower additional measurement of the irradiation creep compliance.
3) Materials of compared data consisted of SiC, different SiC fibers, and even SiC_f/SiC composites. Microstructural differences among various SiC impact on irradiation creep behavior [17]. This can explain the scattered results.

As discussed in ref. [33], irradiation creep on steels and metals has been intensively studied for decades, both experimentally and theoretically, but a detailed understanding has not been achieved. The lack of high quality irradiation creep data on SiC retards the deep understanding of phenomenon and calls for further systematic experimental investigation and complementary modelling study.

4. Summary and conclusion

A newly designed clamping system for ceramic matrix composites was developed. By using this system, the uniaxial tensile loading was successfully applied up to fracture (950 MPa) on a SiC_f/SiC minicomposite.

An Irradiation creep test of a SiC_f/SiC composite was performed by using an in-beam creep device under uniaxial tensile stresses from 40 to 382 MPa during homogeneous helium irradiation at 700°C and 900°C. The creep compliances B_0, i.e. creep rate per dose rate (assuming linear dependence) are of 3.07×10^{-5} $dpa^{-1} \cdot MPa^{-1}$ and 5.43×10^{-5} $dpa^{-1} \cdot MPa^{-1}$ for temperature of 700°C and 900°C, respectively.

Acknowledgements

This work was partial funded by SwissNuclear (Project No. LTR-02) and Natural Science Foundation of China (Project No. 91426304). The authors are grateful to the French Network EMIR for helium irradiation and NEEDS French program for the financial support. The authors thank A. Jankowiak (CEA/SRMA) for discussions about the design of the sample holder. The work was performed within the Swiss Generation IV Program and for a contribution to JPNM/EERA.

Reference

[1] ITER Website: https://www.iter.org/

[2] Gen IV Website: https://www.gen-4.org/gif/

[3] SNETP Website: http://www.snetp.eu/

[4] L.L. Snead, T. Notawa, M. Ferraris, Y. Katoh, R. Shinavski and M. Sawan, Silicon carbide composites as fusion power reactor structural materials, J. Nucl. Mater., 417 (2011) 330-339

[5] T. Koyanagi, Y. Katoh, T. Nozawa, L.L. Snead, S. Kondo, C.H. Henager Jr., M. Ferraris, T. Hinoki, Q. Huang, Recent progress in the development of SiC composites for nuclear fusion applications, J. Nucl. Mater. 511 (2018) 544-555

[6] Akira Kohyama and Hirotatsu Kishimoto, SiC/SiC composites materials for nuclear application, Nuclear Safety and Simulation, 4 (2013) 72-79

[7] Kurt A. Terrani, Accident tolerant fuel cladding development: Promise, status, and Challenges, J. Nucl. Mater. 501(2018)13-30

[8] C. Cozzo and G. Khvostov, "ATF Developments at PSI", in Top Fuel 2018, Prag, Czech Republic, 2018

[9] A Technology Roadmap for Generation IV Nuclear Energy System and Supporting Documents, Issued by the U.S. DOE Nuclear Energy Research Advisory Committee and the Generation IV International Forum, GIF-002-00, December 2002

[10] W. Gauthier and J. Lamon, Delayed Failure of Hi-Nicalon and Hi-Nicalon S Multifilament Tows and Single Filaments at Intermediate Temperatures (500°–800°C), J. Am. Ceram. Soc., 92 [3] (2009) 702–709

[11] R.J. Price, Properties of Silicon Carbide for Nuclear fuel particle Coatings, Nucl. Technol. 35 (1977) 372

[12] R. Scholz, Light ion irradiation creep of SiC fibers in torsion J. Nucl. Mater. 258-263 (1998) 1533

[13] R. Scholz, G.E. Youngblood, Irradiation creep of advanced silicon carbide fibers, J. Nucl. Mater. 283-287 (2000) 372-375

[14] Vani Shankar, Gary S. Was, Proton irradiation creep of beta-silicon carbide, J. Nucl. Mater. 418 (2011) 198–206

[15] Yutai Katoh, Lance L. Snead, Chad M. Parish, Tatsuya Hinoki, Observation and possible mechanism of irradiation induced creep in ceramics, J. Nucl. Mater. 434 (2013) 141–151

[16] Sosuke Kondo, Takaaki Koyanagi, Tatsuya Hinoki, Irradiation creep of 3C–SiC and microstructural understanding of the underlying mechanisms, J. Nucl. Mater. 448 (2014) 487–496

[17] Takaaki Koyanagi, Yutai Katoh, Kazumi Ozawa, Kazuya Shimoda, Tatsuya Hinoki, Lance L. Snead, Neutron-irradiation creep of silicon carbide materials beyond the initial transient, J. Nucl. Mater. 478 (2016) 97-111

[18] R. Naslain, J. Lamon, R. Pailler, X. Bourrat, A. Guette, and F. Langlais, micro/minicomposites: a useful approach to the design and development of non-oxide CMCs. Composites Part A: applied science and manufacturing 30 (1999) 537-547

[19] P. Jung, J. Viehweg, C. Schwaiger, Cooling and temperature stabilizing of thin specimens for mechanical measurements under light ion bombardment, Nucl. Instr. and Meth. 154 (1978) 207

[20] P. Jung, Schwaz and H.K. Sahu, An apparatus for applying tensile, compressive and cyclic stresses on foil specimen during light ion irradiation, Nucl. Instr. and Meth. in Phys. Res. A234 (1978) 331

[21] H.L. Heinisch, L.R. Greenwood, W.J. Weber, R.E. Williford, Displacement damage in silicon carbide irradiated in fission reactors, J. Nucl. Mater. 327 (2004) 175–181

[22] G. Lucas and L. Pizzagalli, *Ab initio* molecular dynamics calculations of threshold displacement energies in silicon carbide, Phys. Rev. B72, (2005) 161202

[23] M. Balat-Pichelin, A. Bousquet, Total hemispherical emissivity of sintered SiC up to 1850 K in high vacuum and in air at different pressures, J. Eur. Ceram. Soc. 38 (2018) 3447–3456

[24] J. Chen, P. Jung, M.A. Pouchon, T. Rebac, W. Hoffelner, Irradiation creep and precipitation in a ferritic ODS steel under helium implantation, J. Nucl. Mater. 373 (2008) 22–27

[25] J. Chen, P. Jung, J. Henry, Y. de Carlan, T. Sauvage, F. Duval, M.F. Barthe, W. Hoffelner, Irradiation creep and microstructural changes of ODS steels of different Cr-contents during helium implantation under stress, J. Nucl. Mater. 437 (2013) 432–437

[26] R.V. Hesketh, A Transient Irradiation Creep in Non-fissile Metals, Phil. Mag. 8(1963)1321

[27] R. Bodet, X. Bourrat, J. Lamm, and R. Naslain, Tensile Creep Behaviour of a Silicon Carbide Fiber with a Low Oxygen Content, J. Mater. Sci. 30 (1995) 661-677

[28] J. Chen, P. Jung, H. Klein, Production and recovery of defects in SiC after irradiation and deformation, J. Nucl. Mater. 258-263 (1998) 1803-1808

[29] A.I. Ryazanov, A.V. Klaptsov, A. Kohyama, H. Kishimoto, Radiation swelling of SiC under neutron irradiation, J. Nucl. Mater. 307–311 (2002) 1107–1111
[30] Z. Zhu, P. Jung, Dimensional changes of Al_2O_3 and SiC, proton irradiated under tensile stress, J. Nucl. Mater. 212–215 (1994) 1081-1086
[31] P. Jung, Atomic displacement function of cubic metals, J. Nucl. Mater. 117 (1983) 70
[32] Frank A. Garner, Irradiation performance of cladding and structural steels in liquit metal reactors, in Materialss Science and Technology edited by R.W. Cahn, P. Haasen, E.J. Kramer, Volume 10A, Weinheim-New York-Basel-Cambridge-Tokyo, VCH, 1993
[33] J. Chen, P. Jung, W. Hoffelner, Irradiation creep of candidate materials for advanced nuclear plants, J. Nucl. Mater. 441 (2013) 688–694

Fig. 1: SiC_f/SiC minicomposite prepared by CVI: (a) sketch (for clarity, only a few fibers out of the 500 that constitute a whole tow are represented) and (b) SEM observation of the failure surface.

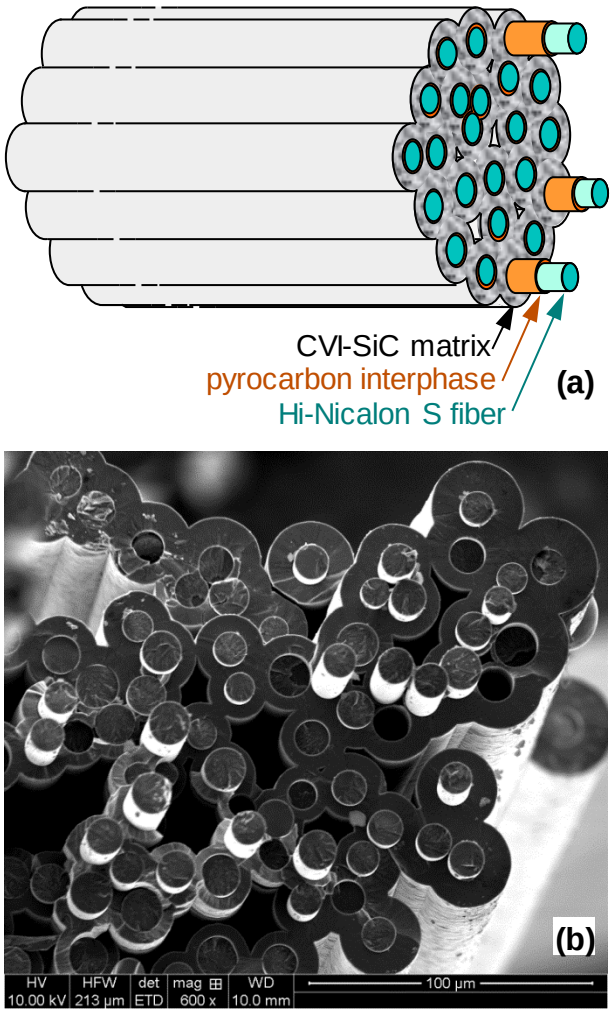

Fig. 2: Ensemble drawing of sample holder: the pink parts are made of graphite and the grey ones of stainless steel. The round sample of SiC_f/SiC minicomposites is indicated by dark red.

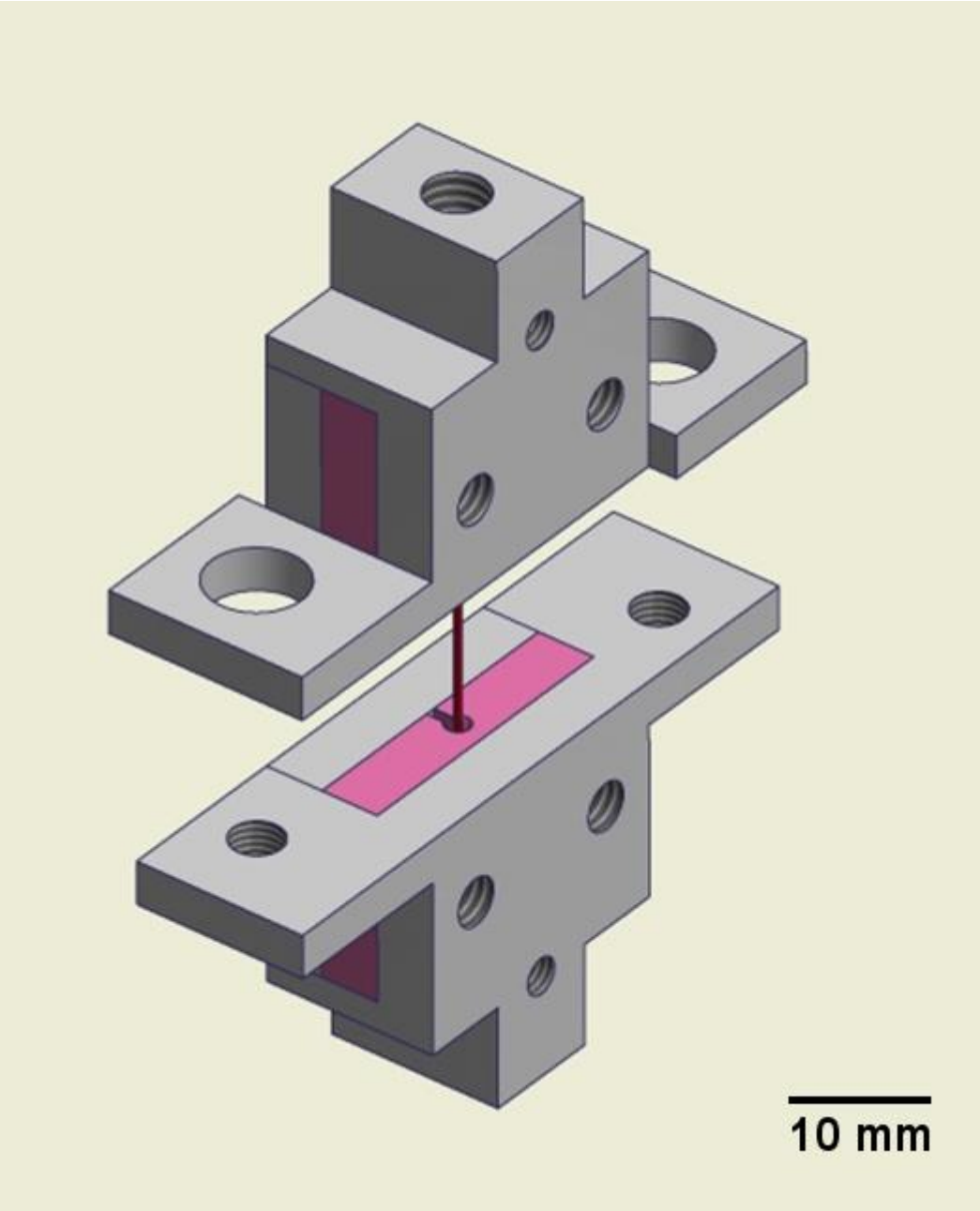

Fig.3: The sketch of in-beam irradiation set up

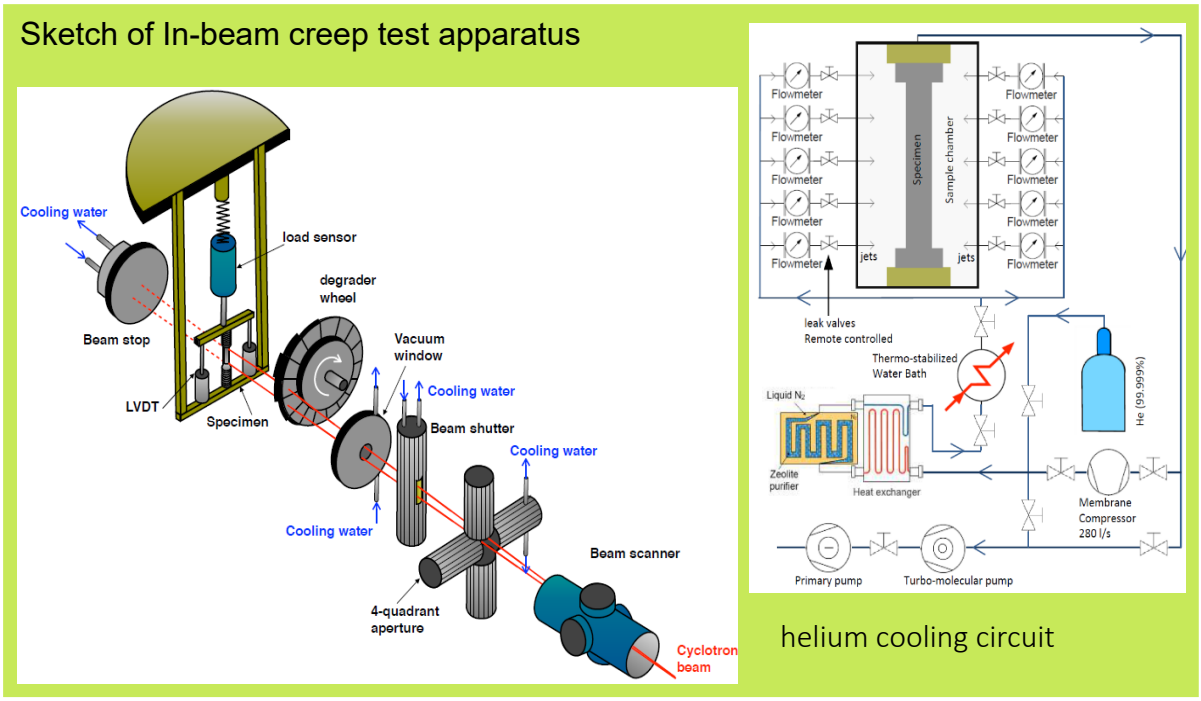

Fig. 4: calculated damage profile of 0 - 45 MeV α beam in SiC by SRIM

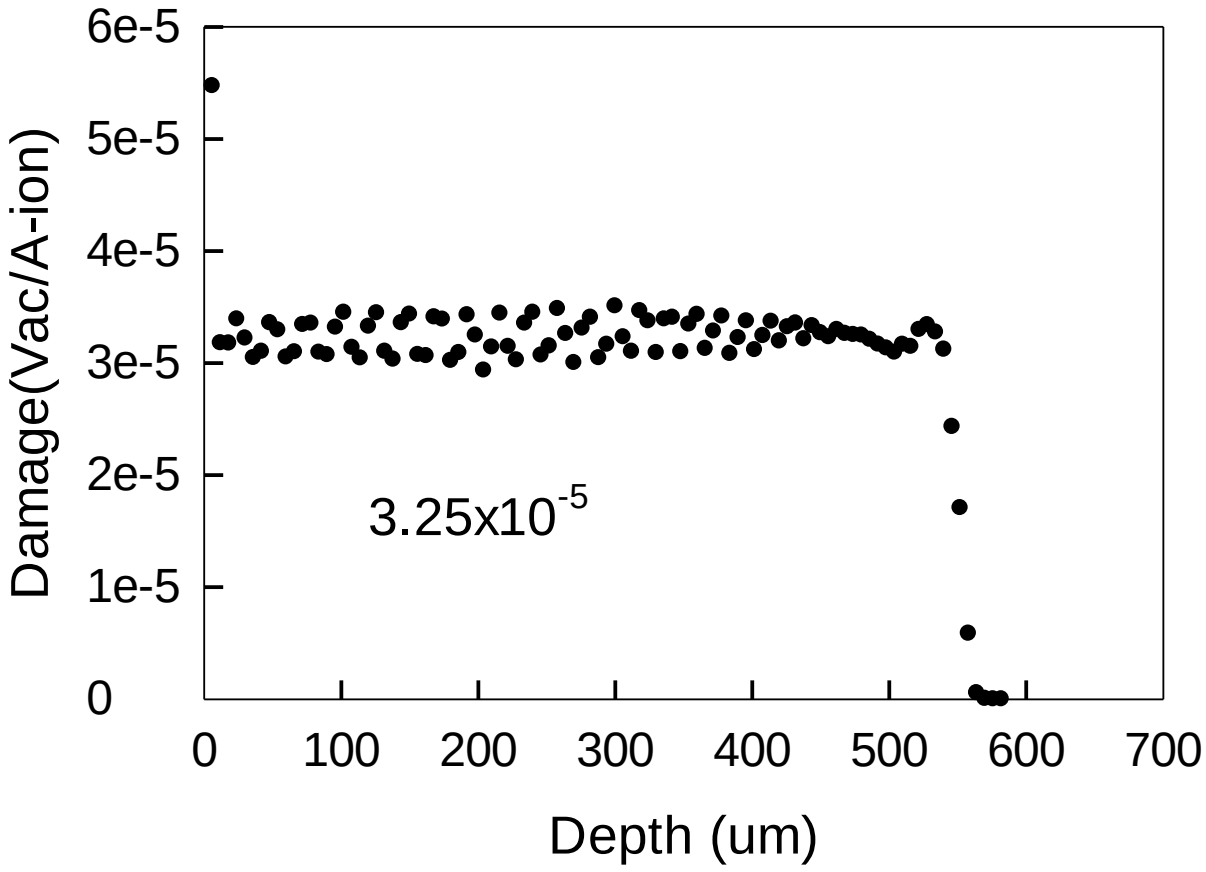

Fig. 5: Measured temperature profile of SiC$_f$/SiC sample. The geometrical center of the sample is defined as position of origin (0), and up direction is positive. The region irradiated by beam located between two arrows (from position -6 to 6).

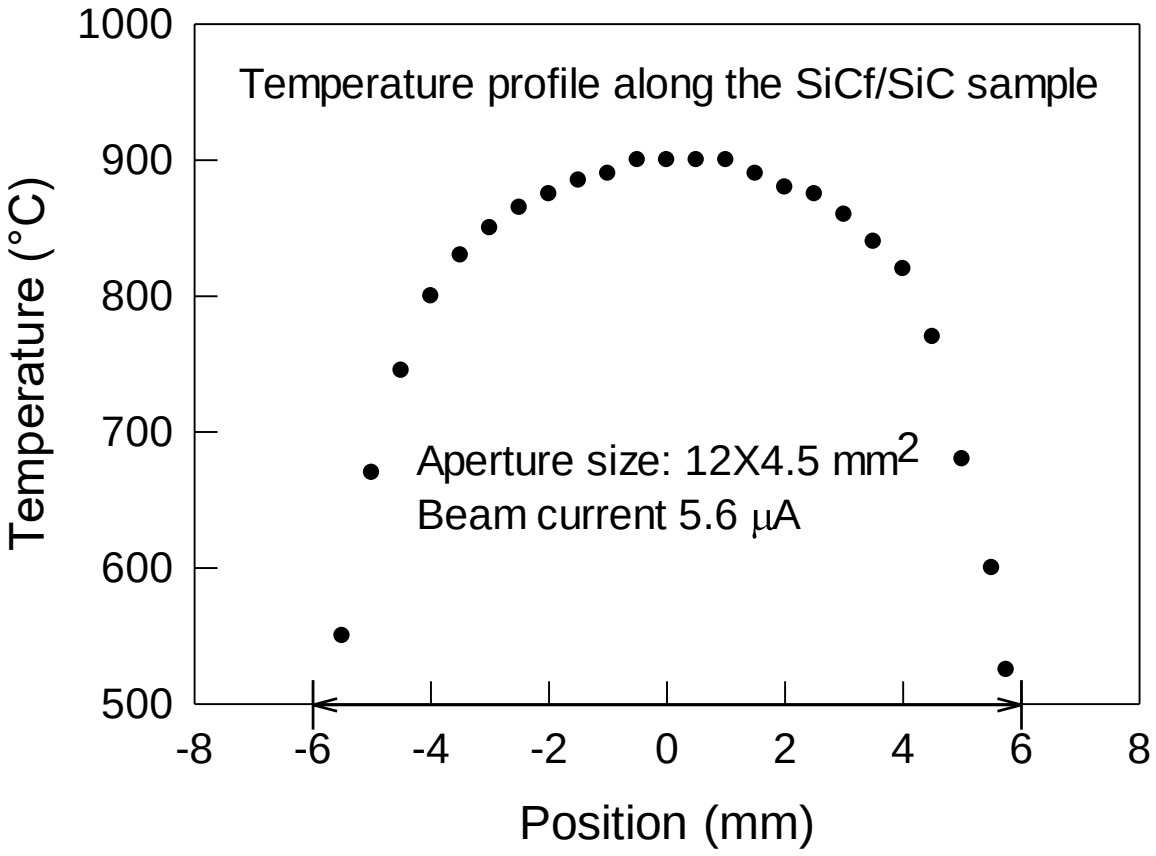

Fig. 6 Tensile curve of SiC_f/SiC minicomposite at 900 °C under helium irradiation

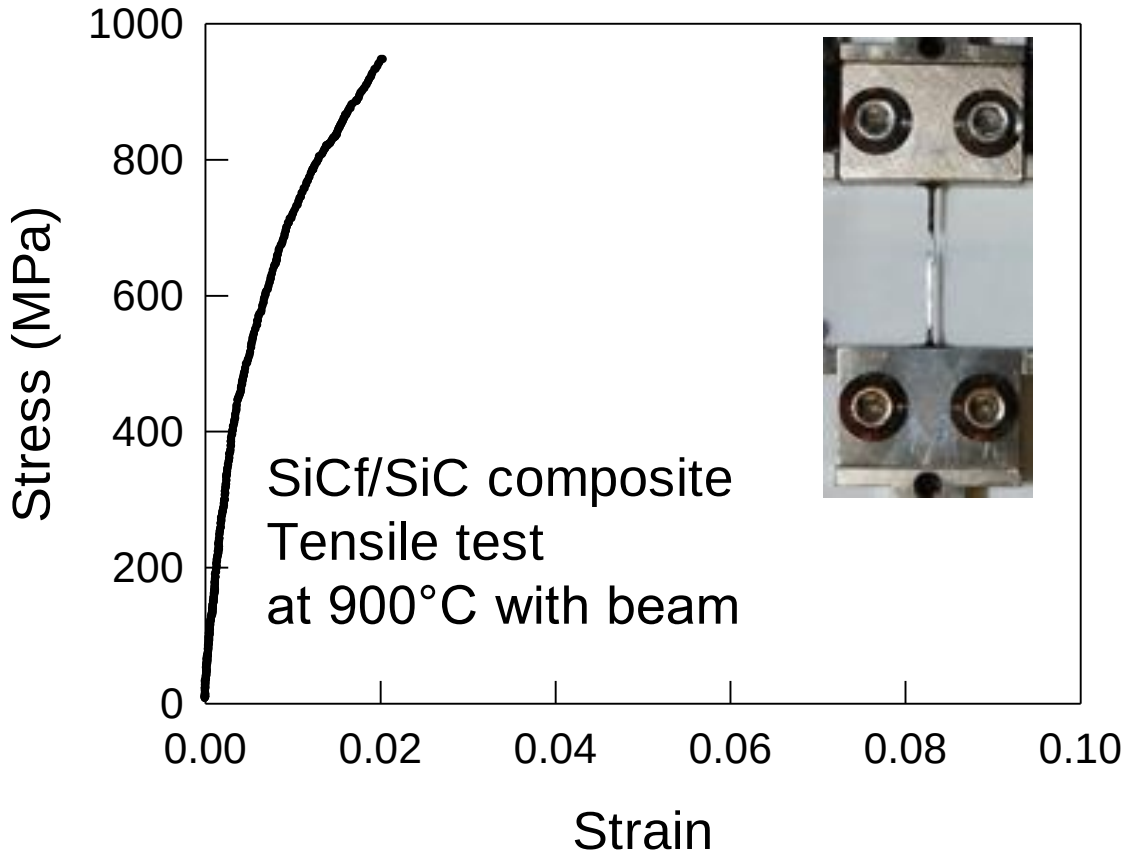

Fig. 7: Length changes monitored during beam-off periods by LVDT as a function of the chamber temperature. All strains were measured at 65°C. 8 successive strain measurements were typically performed every 2 hours of irradiation.

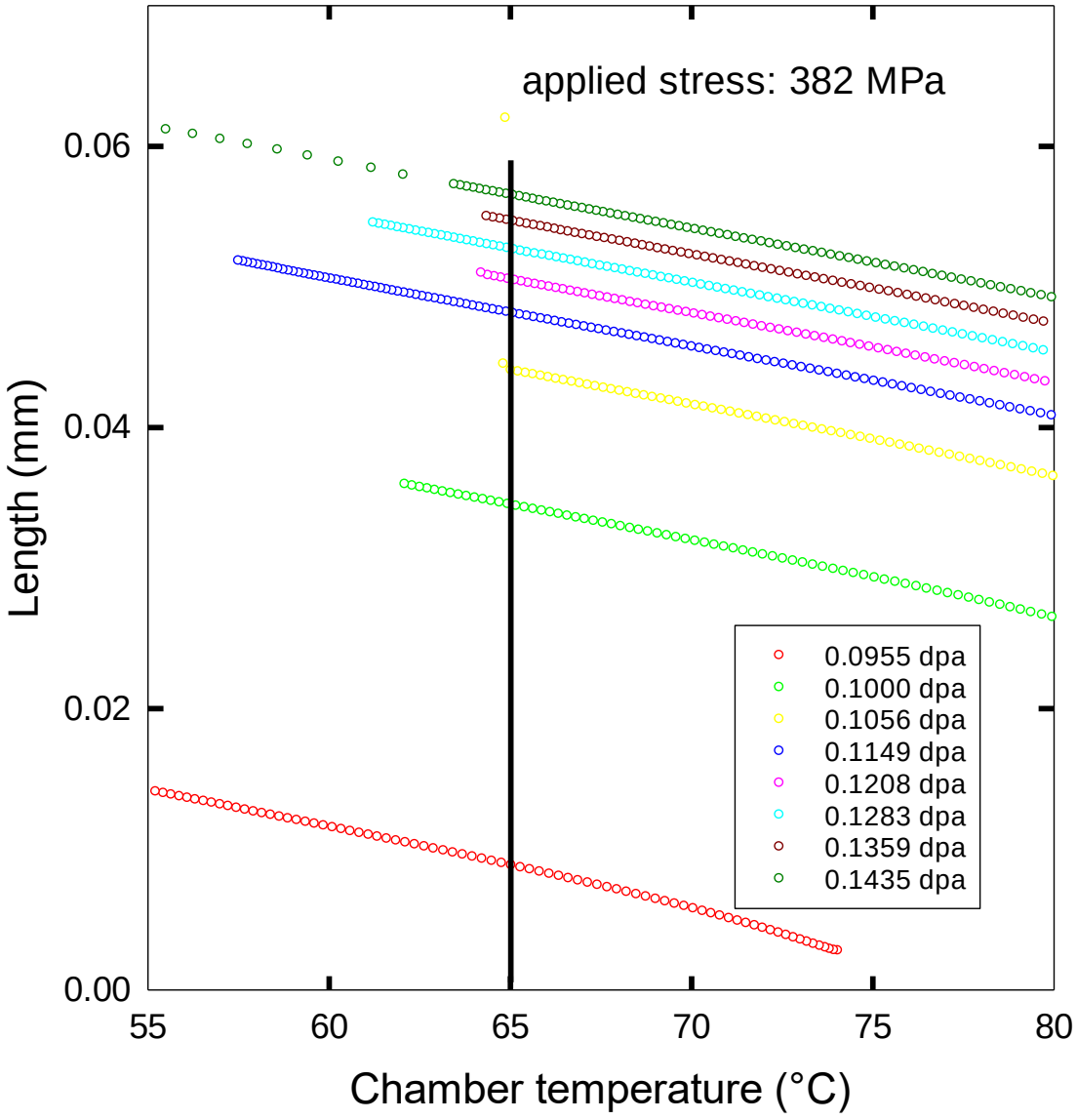

Fig.8: the strain of SiC_f/SiC minicomposite during He-irradiation at 700°C as a function of the displacement dose.

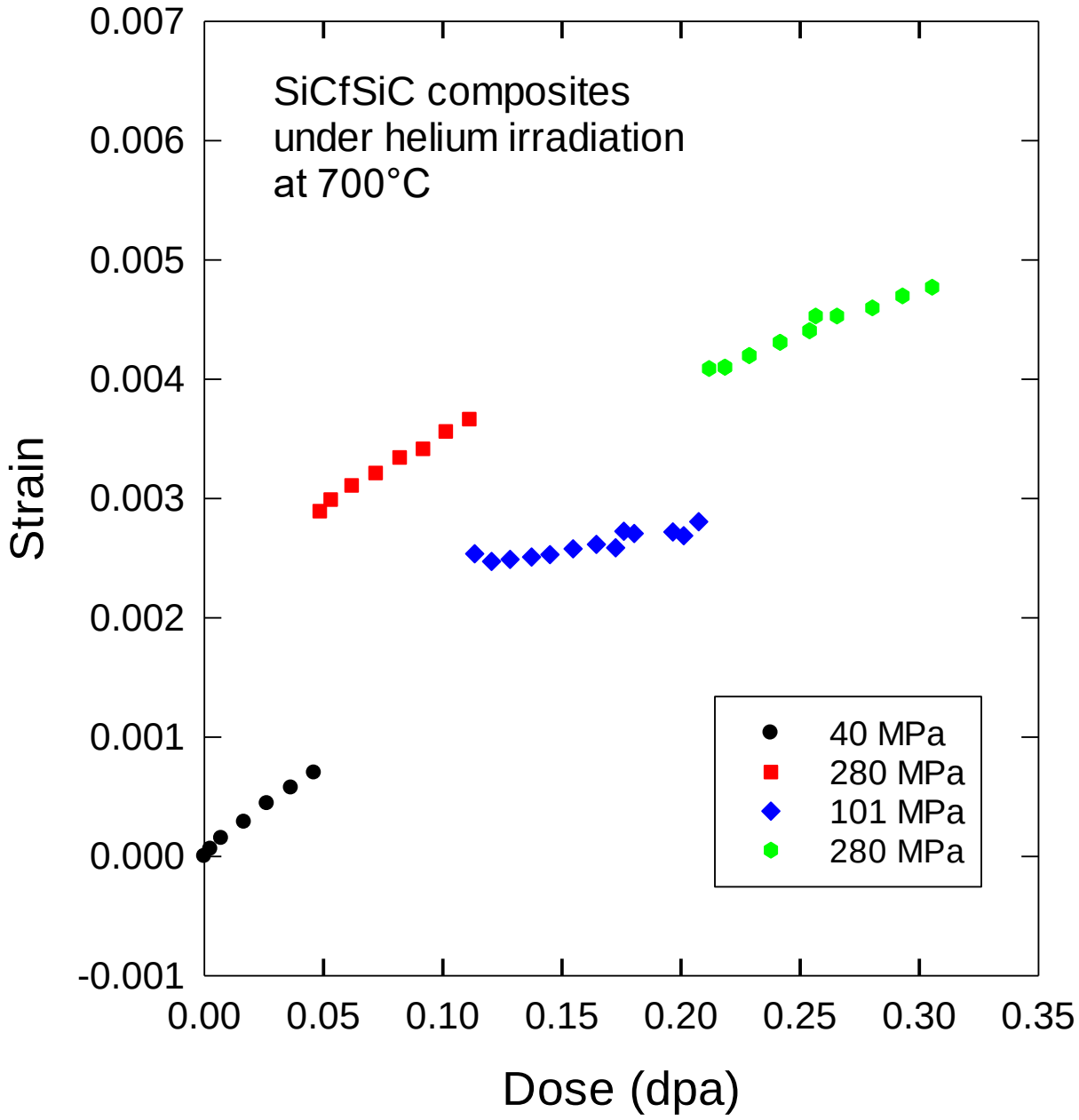

Fig. 9: the strain of SiC$_f$/SiC minicomposite during He-irradiation at 900°C as a function of the displacement dose.

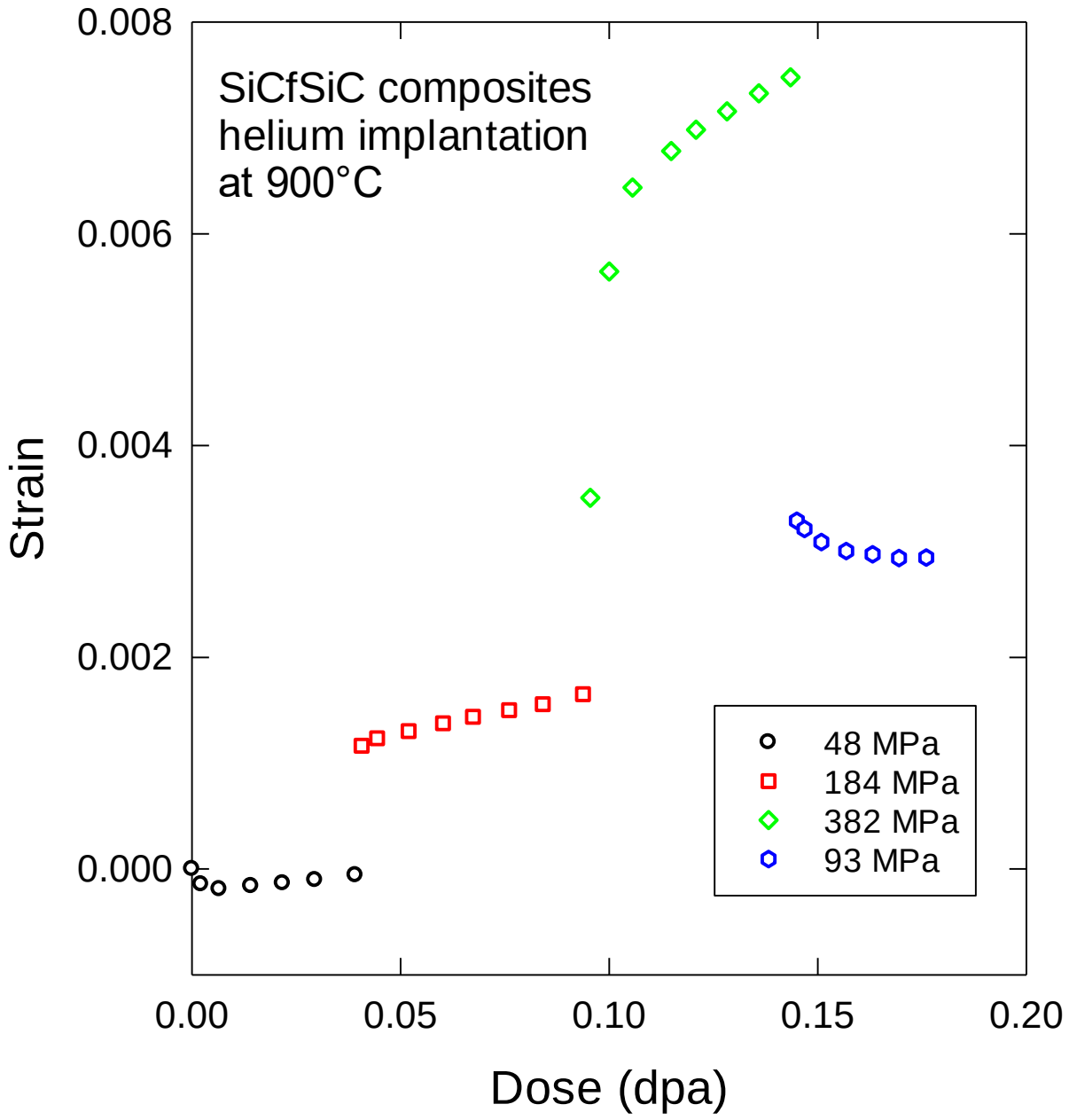

Fig. 10: strain rate/dose rate as a function of stress. Slope of fitting lines give irradiation creep compliances.

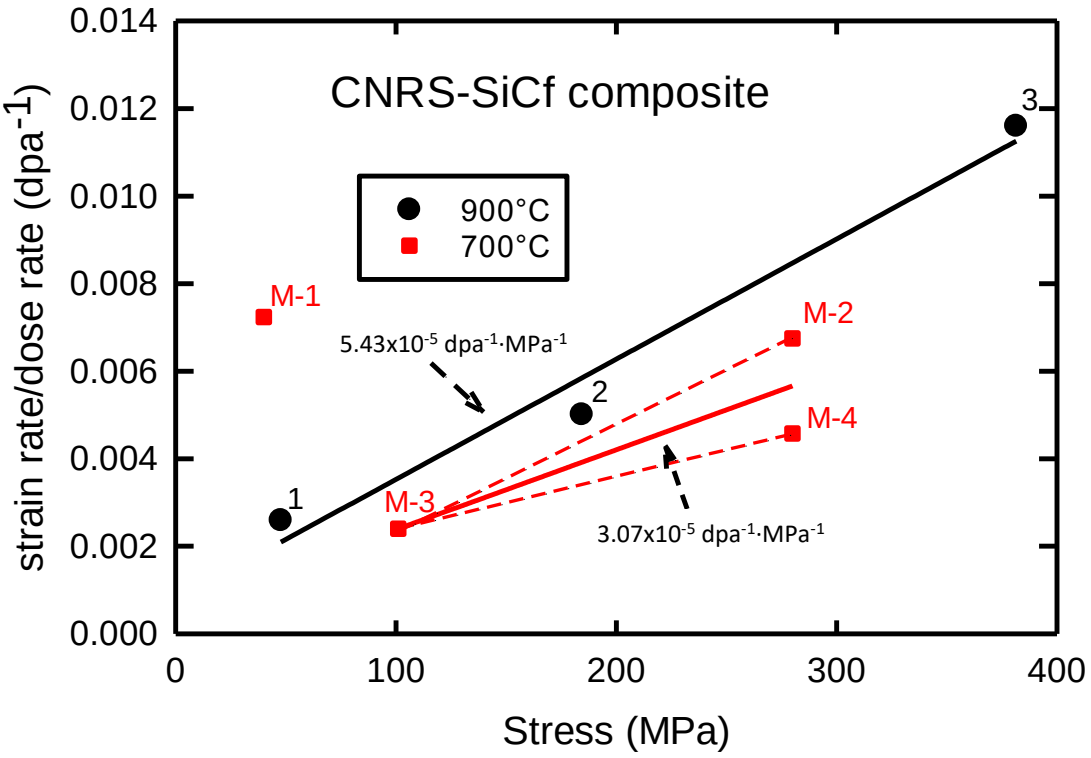

Fig. 11 Comparison of irradiation creep compliance